

## Influence of the number of layers on the equilibrium of a granular packing

M. A. Aguirre, N. Nerone, and A. Calvo

*Grupo de Medios Porosos, Facultad de Ingeniería, Universidad de Buenos Aires, Paseo Colón 850, 1063 Buenos Aires, Argentina*

I. Ippolito and D. Bideau

*Groupe Matière Condensée et Matériaux, UMR 6626, Université de Rennes 1, Campus de Beaulieu, 35042 Rennes Cedex, France*

(Received 28 September 1999)

This paper reports an experimental study on avalanches in a granular material contained in a confined geometry. The granular packing is made of monosize glass beads initially poured into a box that is slowly inclined until an avalanche takes place at a critical angle  $\theta_M$  (maximum angle of stability). The avalanche involves a decrease of the surface slope until a second critical angle  $\theta_r$  (angle of repose) is reached. Both angles and the mass displaced out of the box during the avalanche are studied as a function of the height of the granular packing. In order to avoid cohesion effects, experiments are carried out in a humidity controlled environment. For small packings, up to approximately ten layers, the stability of the system is significantly affected by the rough surface at the bottom. In contrast, for thicker systems, critical angles do not depend on the height.

PACS number(s): 45.70.Ht, 45.70.Mg, 05.45.-a

### I. INTRODUCTION

Granular flows are very important in different industrial processes, like handling, transport, storage, mixing, and the packing of powders, pebbles, sand, gravel, flour, salt, grains, and seeds in pharmaceutical, building, and food industries, for example. On another scale, some geological processes also involve granular systems: avalanches, dune formation, earth-plate displacements, etc.

Surface flows on a sand heap have been the subject of a tremendous number of scientific works [1], particularly in the last ten years following the paper by Bak, Tang, and Wiesenfeld (BTW) [2], which related the surface instability of a sand heap (i.e., avalanches) to self-organized-criticality (SOC). These works have shown that a sand heap is not a good experimental system to test the pertinence of SOC, essentially because the equilibrium of the heap does not depend on only one “critical” angle, as in the cellular automaton described by BTW, but on two angles (at least): (i) the maximum angle of stability  $\theta_M$ , which is here defined as the angle at which, on the average, the avalanche starts and, (ii) the angle of repose  $\theta_r$ , which is the angle at which, on the average, it stops. Fauve and co-workers [3], performing experiments in a rotating drum, found different avalanche regimes depending on the rotation speed of the drum: a chaotic regime at small velocities and a periodic regime at larger ones. They proposed a simple model for avalanches based on an analogy with the stick-slip motion observed in the case of solid friction. This model fits their experimental results very well. More recently, Bouchaud *et al.* ([4,5]) have proposed a new theoretical model for continued surface flow (rather than avalanche-type flow) based on a set of coupled equations relating the moving grain density  $R(x,t)$  and the local height  $h(x,t)$  (where  $x$  is the spatial coordinate and  $t$  is time). A dispersion constant  $D$  is introduced to take into account velocity fluctuations. De Gennes and collaborators [6] have proposed a modified version of this model, without the diffusion term (assumed as negligible). These authors introduce

a neutral angle  $\theta_n$ , defined as the angle at which erosion balances accretion and is uniquely defined (it does not depend on the type of experiment performed; for example, if the avalanche takes place in an open cell, the angle of repose is equal to  $\theta_n$ , whereas in a closed cell the angle  $\theta_r$  is not  $\theta_n$ , but  $\theta_r = \theta_n - \delta = \theta_M - 2\delta$ ). They also distinguish thin flows from thick flows, where saturation effects are present, and analyze downhill and uphill waves due to the convection velocity of the grains within the rolling phase. We observed those uphill and downhill waves in our experiments, but the difference between thin and thick flows turned out to be much more dramatic than predictions.

Pouliquen and Renault [7] have recently studied the onset of a flow of two granular materials resting on a rough bed. The critical angle at which the particles start to flow is found to increase when the initial depth of the pile decreases, showing that the cohesion of the material is greater near the bed than in the bulk. This result is partially confirmed by these experiments because the thickness of the systems used in the experiments herein reported covers a larger range.

Some authors have tried to link  $\theta_M$  to a stability criterion starting from one ball in equilibrium on a triangle of three balls [8]. We shall see that these predictions are not confirmed by our experiments.

This work analyzes the dependence of the stability of a granular packing on its size (number of layers). We are essentially concerned with the dependence of  $\theta_M, \theta_r$ , and the average avalanche mass  $M$  on the thickness of the granular system.

### II. EXPERIMENTAL SYSTEM

Experiments are carried out in a box 32-cm long and 26-cm wide. The box is made of transparent glass that allows the observer to visualize the heap inside.

To obtain a disordered packing, the box is filled up with glass beads ( $2.2 \pm 0.2$  mm in diameter), which are poured over a rough bottom surface. This bottom bed is made by

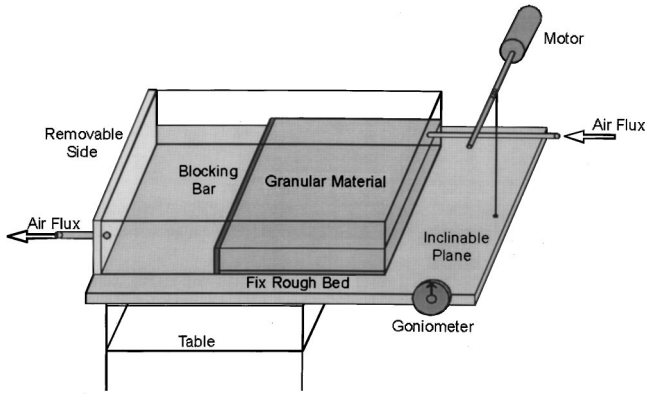


FIG. 1. Experimental setup.

gluing the same glass beads that fill both systems over a flat piece of glass.

Taking into account bead density, the diameter, and the bottom area of the system, the amount of mass needed to form one granular layer with a two-dimensional (2D) packing fraction of 0.7 is determined, a procedure widely used in previous works ([9,10]). The addition of this quantity (230 g) of granular material to the system is counted as adding one layer onto it. This ensures a regular increase in the height of the system. Experimentally, it was found that the packing height  $h$  is a function of the number of layers  $N$ :

$$h \approx \frac{\sqrt{3}}{2} dN, \quad (1)$$

where  $d$  is the bead diameter, and the approximation holds for  $N > 1$ . The factor of proportionality in Eq. (1) is close to the value found for a high closed packing (HCP).

One of the most important experimental problems lies in adjusting the height of the blocking bar at the outlet of the box (see Fig. 1). If the bar is a few centimeters higher than the granular medium, it stops the avalanche, the mass of which cannot then be measured. This may modify both the angle of repose  $\theta_r$ , and the regime of avalanches [11]. If the blocking bar is removed, the slope of the system at this level corresponds to the angle of repose, and the avalanche always starts at this place. Thus the decision was made to place a wall, the upper side of which was leveled with the center of the balls, in the upper layer of the system. With such an arrangement, the wall cannot stop an avalanche, but it stabilizes the packing and decreases the probability that an avalanche may start at a small distance from it [12]. The blocking bar may influence and modify—weakly—the results of the experiments.

From experimental observations, it is clear that the relative humidity of the room air in which the experiment is performed has a great influence. For a relative humidity larger than 60%, capillary forces give cohesion to the medium, and for a relative humidity smaller than 45%, electrostatic forces are at least of the order of the weight of the grains [1]. The most significant experiments were carried out under a controlled humidity of 50% and will be compared to the ones performed at higher room humidity.

To keep humidity at a constant value of 50%, the box that contains the granular material is connected to a slow flow of

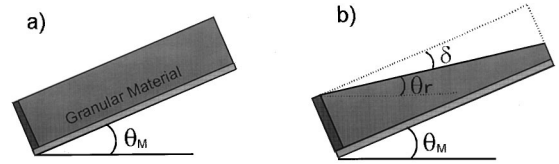


FIG. 2. (a) Maximum angle of stability  $\theta_M$ , where the avalanche begins. (b) Final configuration for a large enough number of layers. White zone corresponds to the total displaced mass during the avalanche.

air, which is filtered to avoid any contamination. The air comes from a closed container with distilled water that is plugged into a thermal bath at a temperature  $T$  below room temperature  $T_a$ . In this container, water is in equilibrium with its vapor and, when the air at temperature  $T$  reaches the box at a higher temperature  $T_a$ , it lowers its humidity. Humidity is measured inside the box by means of a thermohygrometer.

For a system with a given number of layers  $N$ , ten experiments are performed at a fixed humidity value. The number of layers varies between 1 and 34.

The box is secured on a heavy plane apt to be inclined at different angles and initially tilted at an angle with respect to the horizontal that is increased at a rate of  $5^\circ$  per minute, from  $0^\circ$  to  $20^\circ$ , quite far from the value at which avalanches start. When the critical angle  $\theta_M$  is approached (after  $20^\circ$ ), the angle variation rate is slowed down to  $1^\circ$  per minute until a large avalanche is detected.

The avalanche mass  $M$  is measured using an electronic scale connected to a PC computer. The maximum angle of stability,  $\theta_M$ , is measured with a goniometer fixed to the plane [Fig. 2(a)]. To calculate the angle of repose we measure the angle  $\delta$  [Fig. 2(b)] between the plane and the final free surface:  $\theta_r = \theta_M - \delta$ .

When the number of layers of the system is large enough, the angle  $\delta$  can be determined in two ways: (i) by decreasing the angle of the plane till the final free surface of the pile is horizontal and then measuring it directly with a goniometer; (ii) by using the avalanche mass and the final geometry achieved by the system [Fig. 2(b)]:  $\tan(\delta) \propto M$ .

For systems with a fewer number of layers, the final free surface of the packing is not always flat. The way in which we determine  $\delta$  in this case will be explained in Sec. IV A. Finally, mean values  $\langle \theta_M \rangle$ ,  $\langle \theta_r \rangle$ ,  $\langle \delta \rangle$ , and  $\langle M \rangle$  are computed over the ten measurements with fixed  $N$ .

### III. EXPERIMENTAL OBSERVATIONS

Before a large avalanche is produced, small and large surface rearrangements are observed. These rearrangements take place at random locations on the free surface of the packing and may involve from less than 1% of the surface (small rearrangements) to almost the whole free surface (large rearrangements). A detailed study is being carried out on the latter, and results will soon be reported. Preliminary results widely found in the literature show that small rearrangements occur before the angle of repose, and that size distribution follows an exponential law with an exponent around  $-1.5$  ([13,14]). Large rearrangements occur between the angle of repose  $\theta_r$ , and the maximum angle of stability

$\theta_M$ , and they may be detected at a regular step  $\Delta\theta$  that seems to depend on the number of layers of the packing. Their size distribution follows an exponential behavior depending on  $\theta$ .

As for large avalanches, they may also start at any place on the free surface, but very quickly their size increases and becomes of the order of the size of the system. This behavior is comparable to the one reported by Bretz *et al.* [15]. Depending on the thickness of the packing, two kinds of processes may be observed.

#### A. Avalanches in thin granular packings

- (i) The avalanche starts anywhere on the free surface.
- (ii) A bouncing flow takes place where grains interact directly with the fixed rough bed.
- (iii) All layers are involved in the process.
- (iv) Once the avalanche stops, the retained grains form a wedge close to the blocking bar, and sometimes a small portion gets randomly trapped in the rough bottom. In those cases,  $\delta$  is not well defined and it cannot be directly measured with the goniometer. However, an effective angle  $\delta_{\text{eff}}$  can be estimated using the avalanche mass (Sec. IV A).

#### B. Avalanches in thick granular packings

(i) Avalanches also start anywhere on the free surface. At the onset of the avalanche, a few grains start to roll down, but very quickly the movement is amplified because rolling grains destabilize some other grains. Depending on the starting location of the avalanche, two kinds of amplification processes are observed:

(a) The avalanche starts near the top of the free surface. Grains start to roll downhill from this location, and a destabilizing wave propagates downward until it reaches the bottom.

(b) The avalanche starts somewhere in the middle or in the lowest part of the box. Grains also start to roll down and flow out of the box but, in addition, an uphill wave may be observed, involving new grains that start to roll.

(ii) Not all layers are involved in the process. In fact, the most remarkable experimental observation is that only grains belonging to a fixed number of superficial layers are set into motion. That is, independently of the height of the packing, a constant number of superficial layers contribute to the avalanche process. This critical number of layers is herein called  $N_c$ .

(iii) In particular, it is very interesting to remark the way in which these  $N_c$  layers are set into motion. As stated above, the process begins at the free surface. Almost immediately, the second layer begins to move, then the third one, and so on, up to approximately the fifth one. At this point, the first layer has already flown out of the box. Propagation proceeds inside the bulk while superficial layers are removed from the system. In this way, one can always observe a creeping band of approximately five layers in motion. When the perturbation reaches layer  $N_c$ , the avalanche stops.

(iv) Once the avalanche stops, the final free surface of the system becomes flat and extends over the full length and width of the box leaving an empty volume that is almost a perfect wedge of angle  $\delta$ . Figure 3 shows a lateral view of the free surface after the avalanche stopped.

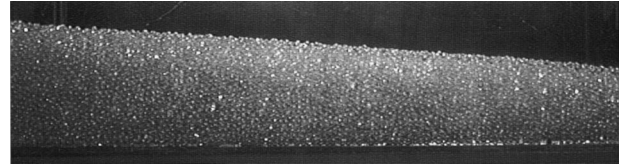


FIG. 3. Lateral view of the final free surface in a 34-layer system after the avalanche stopped. The inclinable plane is horizontal and the avalanche took place to the left side of the box.

(v) Finally, the metastable zone, between the angle of repose  $\theta_r$  and the maximum angle of stability  $\theta_M$ , reported in several works ([4,5]), was not found in the system herein reported. In order to study the stability of the packing in this zone, a set of experiments was performed: the plane was raised at a constant velocity and smoothly stopped every  $5^\circ$  before the angle of repose,  $\theta_r$ , was reached, and every  $1^\circ$  beyond. Each time, the system was exposed to both weak and strong perturbations: blocks of two different weights were thrown from a constant height on the table that held the granular packing. Three different behaviors were found:

(a) For  $\theta < \theta_r$ , small rearrangements were observed following the external perturbation.

(b) For  $\theta_r < \theta < 24.5^\circ$ , the system still remained very stable with respect to external perturbations, which triggered large surface rearrangements that did not evolve into an avalanche.

(c) For  $24.5^\circ < \theta < \theta_M$ , large surface rearrangements originated by an external perturbation led to an avalanche.

## IV. EXPERIMENTAL RESULTS

In this section, experimental results are reported. In Sec. IV A, the behavior of  $\theta_M$  and  $\delta$  for a fixed number of layers is studied. Later on, the variation of mean values  $\langle M \rangle$ ,  $\langle \theta_M \rangle$ , and  $\langle \delta \rangle$  with the number of layers  $N$  is discussed. In Sec. IV C, the influence of humidity is analyzed.

### A. Determination of $\theta_M$ and $\delta$ in a system with a fixed number of layers

As stated above for a packing with a certain number of layers  $N$ , several experiments were performed under identical conditions. In each experiment, the maximum angle of stability  $\theta_M$ , the mass of the avalanche  $M$ , and the angles  $\delta$  or  $\delta_{\text{eff}}$  were measured. In order to make a good determination of these typical values, ten experiments performed under identical conditions turned out to be enough. Very interesting results were obtained from the analysis of these ten measurements. The results obtained for thick and thin packings are described under separate headings. The critical number of layers separating both regimes is  $N_c \approx 13$ .

#### 1. Thick packings ( $N > N_c$ )

Figure 4 shows the ten measurements obtained in a 20-layer system. The maximum angle of stability  $\theta_M$  and  $\delta$  are plotted as a function of the avalanche mass.

Avalanches do not start exactly at the same angle  $\theta_M$ ; the values fluctuate within a certain range, typically  $3^\circ$ , with corresponding fluctuations of the avalanche mass. Similar results were obtained by Pouliquen and Evesque ([7,16]),

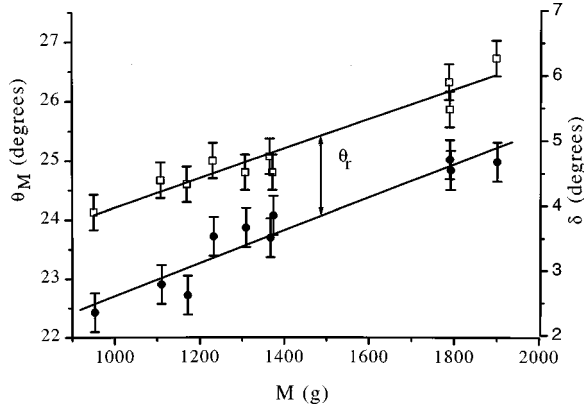


FIG. 4.  $\theta_M$  (open squares) and  $\delta$  (filled circles) as a function of the avalanche mass  $M$  obtained in a 20-layer packing and fitting curve (filled lines).

who ascribe the dispersion to the initial random packing. The same fluctuation is found for  $\delta$  values. However, within these fluctuations a strong correlation is found between the mass of a given avalanche and the corresponding values of  $\theta_M$  and  $\delta$ .

The linear dependence between  $\delta$  and  $M$  might be expected because both variables are representative of the size of the avalanche [Fig. 2(b) and Eq. (1)]:

$$\tan(\delta) \approx \delta = \frac{\sqrt{3}d}{mL} M, \quad (2)$$

where  $d = (2.2 \pm 0.2)$  mm is the bead diameter,  $m = (230 \pm 1)$  g is the mass of one layer, and  $L = (320 \pm 2)$  mm is the box length. These values lead to a factor of proportionality in Eq. (2) of  $(52 \times 10^{-3} \pm 6 \times 10^{-3}) \text{ kg}^{-1}$ , while the slope of the linear regression shown in Fig. 4 is  $53 \times 10^{-3} \pm 8 \times 10^{-3} \text{ kg}^{-1}$ . A similar agreement is obtained for all the systems under study having  $N > N_c$ .

As may be seen in Fig. 4,  $\theta_M$  also displays a linear behavior with respect to the avalanche mass, and both straight lines have roughly the same slope. Considering  $\theta_M = \theta_r + \delta$  and Eq. (2), this result shows that once the avalanche starts at some angle  $\theta_M$ , the process evolves, displacing a quantity  $M$  out of the packing of mass such that the free surface always reaches the same angle  $\theta_r$ , whatever the values of  $\theta_M$  and  $M$ . The same behavior is obtained for the values of  $N > N_c$  considered in this work. In other words,  $\theta_r$  appears to be an intrinsic parameter of the granular medium, as generally expected in the literature [18].

## 2. Thin packings ( $N < N_c$ )

Systems with less than  $N_c$  layers are analyzed in this section. Figure 5 shows the variation of  $\theta_M$  with  $M$  for a series of ten measurements performed on a six-layer packing. Again,  $\theta_M$  fluctuates within a range of  $3^\circ$ , but in this case the dependence on  $M$  is not linear.

It should be remembered that for  $N < N_c$ ,  $\delta$  is sometimes not defined, and it cannot be directly measured with a goniometer. However, an effective angle  $\delta_{\text{eff}}$  can be computed if one supposes that the retained mass always accumulates close to the blocking bar, forming a wedge of angle  $\delta_{\text{eff}}$  as shown in Fig. 6. Then the following geometrical relation between  $\delta_{\text{eff}}$  and the avalanche mass  $M$  holds:

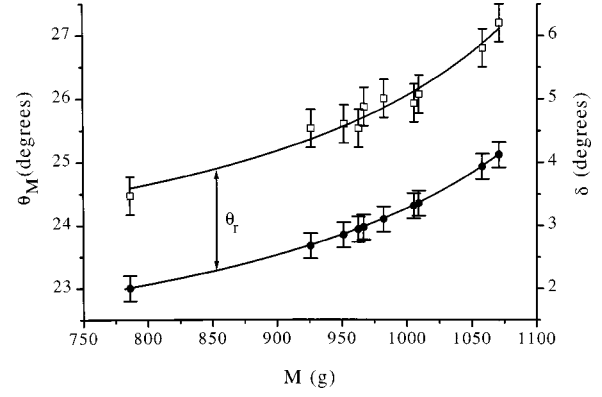


FIG. 5.  $\theta_M$  (open squares) and  $\delta$  (filled circles) as a function of the avalanche mass  $M$  obtained in a six-layer packing and fitting curve (filled line).

$$\tan(\delta_{\text{eff}}) \approx \delta_{\text{eff}} = \frac{\sqrt{3}dm}{4L} \frac{N^2}{(mN - M)}. \quad (3)$$

In Fig. 5,  $\delta_{\text{eff}}$  values computed from Eq. (3) are plotted, with  $N = 6$  and measured mass values. As may be seen, both curves display the same trend, the difference between them being a constant value which, as shown in Fig. 6, is  $\theta_r$ .

In short, for a packing with a given number of layers  $N$ , an avalanche is observed for different values of  $\theta_M$  within a certain range. This range spreads over approximately  $3^\circ$ . However, despite this dispersion, the larger the angle  $\theta_M$  at which the avalanche starts, the larger the mass  $M$  displaced out of the box, so that the final free surface always reaches the same angle  $\theta_r$ . Section IV B reports on the variation of  $M$ ,  $\theta_M$ ,  $\theta_r$ , and  $\delta$  mean values with the number of layers of the packing.

## B. Influence of the number of layers

### 1. Avalanche mass

Figure 7 displays variations of the mean avalanche mass  $\langle M \rangle$  with the number of layers of the packing. The plot corroborates the existence of a critical number of layers  $N_c$  that separate two different behaviors of the avalanche mass.

(i) Up to  $N = N_c \approx 13$ , the mean mass of the avalanche increases with the number of layers of the system.

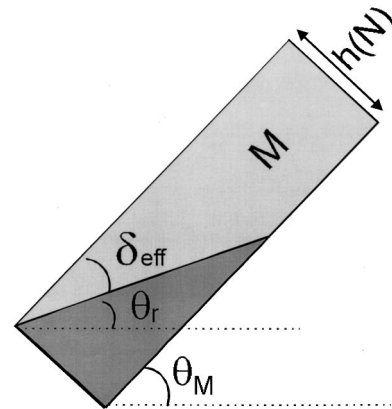


FIG. 6. Scheme of the final packing configuration for  $N < N_c$ .

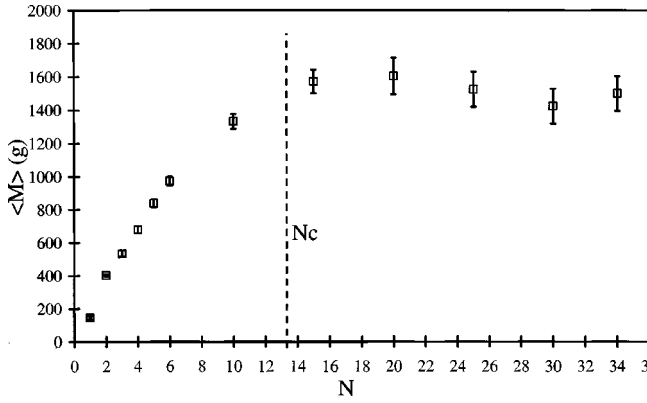


FIG. 7. Mean avalanche mass as a function of the number of layers of the system.

(ii) For  $N > N_c$ , the mass of the avalanche is almost constant  $\langle M \rangle = (1524 \pm 70)$  g and the final free surface of the system is flat (the wedge is reached). It should be recalled that in this regime, only  $N_c$  superficial layers are involved in the avalanche. Then  $N_c$  can be calculated considering that the avalanche mass is the one contained in half the parallelepiped formed by these  $N_c$  layers:

$$\langle M \rangle = \frac{1}{2} m N_c. \quad (4)$$

Using experimental values for  $\langle M \rangle$  and  $m = 230$  g, the following value is obtained:  $N_c = 13 \pm 1$ , which agrees with visual observation.

### 2. Maximum angle of stability

Figure 8 displays values of the mean maximum angle of stability,  $\langle \theta_M \rangle$ , and the angle of repose,  $\langle \theta_r \rangle$ , for different number of layers. For  $\langle \theta_M \rangle$ , three regimes are observed depending on the number of layers of the granular packing:

(i) For packings with less than four layers, when the number of layers increases (from one to four) the system becomes more unstable, entailing a decrease in  $\langle \theta_M \rangle$ . This fact is related to the dilatancy of the packing: for systems with few layers the rigidity of the fixed rough bed imposes a greater level of dilatancy, leading to a more stable system. As the number of layers is larger, this constraint gets weaker allowing an easier displacement of grains. Nevertheless, as

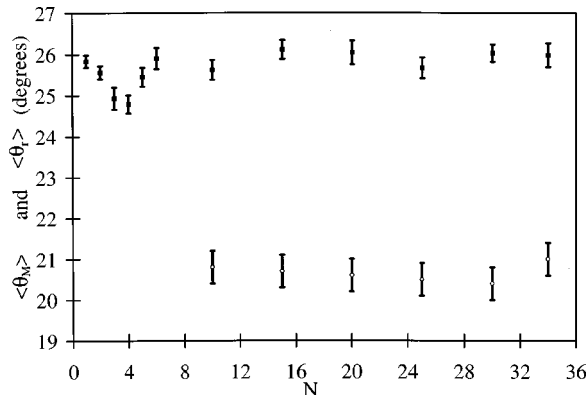


FIG. 8. Mean maximum angle of stability (filled squares) and mean angle of repose (open circles) as a function of the number of layers of the granular system.

the system gets larger and denser, the significance and influence of this dilatancy effect decreases (is “shielded”) and the following regime holds.

(ii) Between roughly four and six layers, the slope of the curve changes. This change may be due to an increase in the granular system packing fraction, which leads to an increase in the dilatancy required to destabilize the system ([16,17]). Thicker systems are more packed and therefore more stable.

(iii) If the number of layers becomes larger than 6,  $\langle \theta_M \rangle$  does not vary with  $N$ . It reaches instead a constant value  $\langle \theta_M \rangle = 25.9^\circ \pm 0.2^\circ$ .

One curious feature is the fact that the individual static angle  $\theta_s$ , defined as the average angle at which a ball located on the rough surface loses its equilibrium, is significantly larger than  $\theta_M$ .  $\theta_s$  is easily measured by placing a row of beads on the fixed rough bed and increasing the angle of the plane until they get destabilized. Under the conditions of the current experiment, it was found that  $\langle \theta_s \rangle = 35^\circ \pm 7^\circ$ . This result shows that this stability criteria cannot be used to calculate  $\theta_M$  as was suggested by Albert [8]. Moreover, it clearly shows that the surface equilibrium (and the loss of equilibrium) of a heap is a collective effect.

### 3. Angle of repose

For both regimes the angle of repose was defined as  $\theta_r = \theta_M - \delta$ . It should be remembered that for  $N < N_c$  sometimes  $\delta$  was not defined and in such cases  $\delta_{\text{eff}}$  was used, the angle that the free surface would form assuming the mass retained in the box filled a wedge close to the blocking bar. Under this assumption, both  $\langle \theta_M \rangle$  and  $\langle \theta_r \rangle$  were plotted in Fig. 8.

It can be seen that  $\langle \theta_r \rangle$  decreases with  $N$  up to  $N = 10$ . For  $N > 10$ , it remains almost constant and roughly equal to  $21.1^\circ \pm 0.4^\circ$ . This result may be compared to the one obtained by Pouliquen and Renault [7] in a quite different situation: a constant flow of material is poured over a rough plane while it is tilted down until the flow stops. They also found that the angle of repose decreases with increasing granular layers until  $N$  is approximately equal to 10.

It is interesting to compare both curves,  $\theta_M$  and  $\theta_r$ . Whereas, for packings with few layers,  $\theta_M$  decreases and then increases due to the influence of the rough bed and the packing fraction,  $\theta_r$  decreases monotonically. Therefore once the system is set into motion, it evolves toward an angle that is only affected by the fixed rough bed. As the number of layers increases, the influence of the rough bed diminishes and becomes negligible for systems with more than ten layers.

### 4. $\langle \delta \rangle$ angle

Figure 9 shows the variation of  $\langle \delta \rangle$  ( $\langle \delta_{\text{eff}} \rangle$ ) with the number of layers. It can be seen that for  $N < 10$ ,  $\langle \delta_{\text{eff}} \rangle$  increases with  $N$ , while for  $N > 10$ ,  $\langle \delta \rangle$  reaches a constant value.

### C. Influence of humidity

Finally, and in order to evidence the importance of performing these experiments in a humidity controlled atmosphere, the same experiments were performed using an open box under air humidity ranging from 67% to 74%. In Fig. 10, the mean maximum angles of stability for controlled and

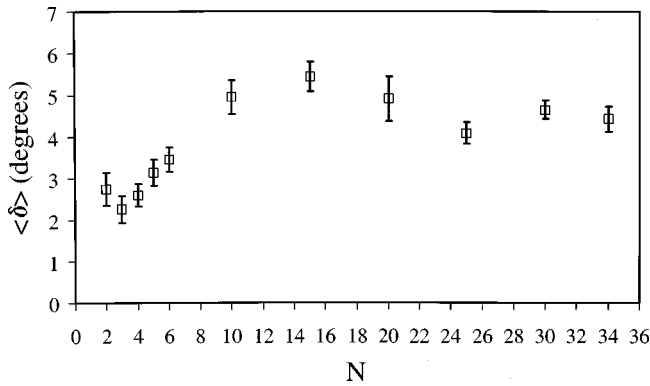


FIG. 9. Avalanche size  $\langle \delta \rangle$  as a function of the number of layers.

variable humidity experiments are shown. Experiments performed at two different approximate humidities show the same qualitative behavior. Nevertheless, an important difference in the stability of the packing is shown. The humid system displays larger variations and remarkably larger angles due to the more cohesive nature of the system. One curious result is that for systems with more than ten layers, the angle  $\delta$  turned out to be the same:  $\langle \delta \rangle_{70\%} = 4.7^\circ \pm 0.8^\circ$  and  $\langle \delta \rangle_{50\%} = 4.7^\circ \pm 0.5^\circ$ . It is not the aim of this work to study the influence of humidity on critical angles. However, in this particular case, the cohesive effect due to humidity affects both  $\theta_M$  and  $\theta_r$  in such a way that  $\delta$  is the same. In order to obtain a conclusive result a larger range of humidities should be explored.

## V. CONCLUSIONS

Our experiments have clearly shown that surface flow and avalanches depend strongly on the height of the packing:

- (i) There is a given height (or a given number of layers  $N_c$ ) above which avalanche characteristics are independent of the packing height.
- (ii) Avalanche dynamics develops according to two different regimes corresponding to thin and thick grain packings. The thin packing regime shows an avalanche process that behaves like a bouncing flow, while the other regime is that of creeping flow. A transition zone is also observed. For

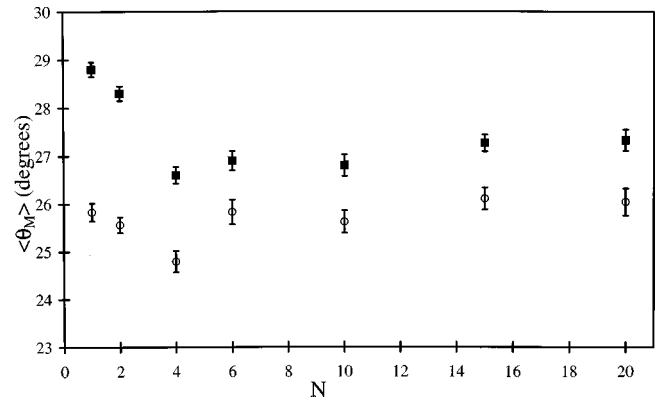


FIG. 10. Mean maximum angle of stability as a function of the number of layers for systems with different degrees of humidity, around 70% (filled squares) and 50% (open circles).

a system with constant height, a strong correlation with the avalanche mass is found for  $\theta_M$  and  $\delta$ .

As observed by Pouliquen and Renault [7], the roughness of the bottom strongly influences the critical angles. In fact, experiments are in progress to study this effect.

$\langle \theta_M \rangle$  values depend on humidity, but the same qualitative results, due to dilatancy effects, were observed for all the packings under study, independent of humidity. Also,  $\langle \delta \rangle$  seems to be independent of humidity.

One of the most relevant results is that the parameters apt to characterize the system in terms of avalanches are  $\theta_r$  (Sec. IV A) and the geometrical parameters. This angle of repose appears to be essential to characterizing surface flow properties of a granular medium.

Experiments are in progress to study the influence of the length of the granular packing. Preliminary results show that the critical number of layers  $N_c$  depends on its length. On the contrary, the angle of repose  $\theta_r$  does not depend on it.

## ACKNOWLEDGMENTS

The authors are grateful for the most valuable collaboration of J. P. Hulin. This work was supported by Ecos-Sud A97-E03, PICS CNRS-CONICET 561, and TI-07 SECyT UBA. One of the authors (D. B.) also received financial support from FIUBA.

- 
- [1] J. Duran, *Sables, Poudres et Grains* (Eyrolles Sciences, Paris, 1997).
  - [2] P. Bak, C. Tang, and K. Wiesenfeld, *Phys. Rev. Lett.* **59**, 381 (1987).
  - [3] M. Caponeri, S. Douady, S. Fauve, and C. Laroche, in *Mobility Particulate Systems*, Vol. 287 of *NATO Advanced Institute, Series E*, edited by E. Guazzelli and L. Oger (Kluwer Academic Publishers, Cargèse, 1995).
  - [4] J. P. Bouchaud, M. E. Cates, J. R. Prakash, and S. F. Edwards, *J. Phys. I* **4**, 1383 (1995).
  - [5] J. P. Bouchaud, M. E. Cates, and P. Claudin, *J. Phys. (France)* **5**, 639 (1995).
  - [6] P. G. de Gennes, *C. R. Seances Acad. Sci., Ser. B* **321-IIIb**, 501 (1995).
  - [7] O. Pouliquen and N. Renault, *J. Phys. II* **6**, 923 (1996).
  - [8] R. Albert, I. Albert, D. Hornbaker, P. Schiffer, and A. L. Barabasi, *Phys. Rev. E* **56**, R6271 (1997).
  - [9] F. X. Riguidel, Ph.D. thesis, Université de Rennes 1, 1994.
  - [10] L. Samson, Ph.D. thesis, Université de Rennes 1, 1997.
  - [11] T. Boutreux, E. Raphael, and P. G. de Gennes, *Phys. Rev. E* **58**, 4692 (1998).
  - [12] F. Cantelaupe, Y. Limon-Duparcmeur, D. Bideau, and G. Ristow, *J. Phys. I* **5**, 585 (1995).
  - [13] K. Lauritsen, S. Zapperi, and H. Stanley, *Phys. Rev. E* **54**, 2483 (1996).
  - [14] L. Amaral and K. Lauritsen, *Phys. Rev. E* **54**, 4512 (1996).
  - [15] M. Bretz, J. B. Cunningham, P. L. Kurczynski, and F. Nori, *Phys. Rev. Lett.* **69**, 2431 (1992).
  - [16] P. Evesque, D. Fargeix, P. Habib, M. P. Luong, and P. Porion, *Phys. Rev. E* **47**, 2326 (1993).
  - [17] S. R. Nagel, *Rev. Mod. Phys.* **64**, 321 (1992).
  - [18] Y. Grasselli and H. J. Herrmann, *Physica A* **246**, 301 (1997).